

Efficient loading and cooling in a dynamic optical evanescent-wave microtrap

PETER DOMOKOS(*) and HELMUT RITSCH(**)

Institut für Theoretische Physik, Universität Innsbruck - Technikerstr. 25, A-6020 Innsbruck, Austria

PACS. 32.80.Pj – Optical cooling of atoms.

PACS. 42.50.Vk – Mechanical effects of light on atoms.

PACS. 42.55.Sa – Microcavity and microdisk lasers.

Abstract. – We calculate the loading efficiency and cooling rates in a bichromatic optical microtrap, where the optical potentials are generated by evanescent waves of cavity fields at a dielectric–vacuum interface. The cavity modified nonconservative dynamic light forces lead to efficient loading of the atoms as well as cooling without the need for spontaneous emission. Steady–state temperatures well below the trap depth, reaching the motional quantum regime, yield very long capturing times for a neutral atom.

Evanescent waves constitute an essential ingredient in various atom optical elements, such as mirrors [1] for gravitational atom optical cavities [2, 3] and for matter waveguides [4], or in optical surface traps [5, 6]. The electromagnetic radiation field experiencing total internal reflection at a dielectric–vacuum interface penetrates into the vacuum with an exponentially decaying field amplitude. Large intensity gradient occurs close to the surface. The resulting optical dipole force on neutral atoms is unusually large and spatially well localized.

In extension of the simple repulsive geometry used for mirrors, Ovchinnikov et al. [7] proposed a wavelength-size optical microtrap based on the evanescent field of *two* radiation modes with different spatial dependence. A strongly red detuned field with a mode function proportional to $\exp(-kx)$ yields a long-range attractive force towards the surface and a second short-range blue detuned field decaying as $\exp(-2kx)$ provides for a short-range repulsive wall. The combination of these two fields generates a tiny but deep trap with a Morse-type potential. Such a trap has a number of remarkable features and potential applicabilities, e.g., it is suitable for studying the interaction between cold atoms and a surface [8], or realizing 2D quantum gas. For a fixed given field configuration the potential is conservative and one can expect long trapping times. However, an efficient loading and cooling mechanism is needed to fill the trap. In the case of the gravito-optical surface trap [5], for example, optical pumping between hyperfine states is applied to implement a Sisyphus-type cooling on the bouncing cesium atoms [9, 10]. The waveguide for argon atoms in [6] also resorts to local optical pumping to achieve an incoherent transfer to a trapped metastable state. In all of these mechanisms

(*) On leave from the Research Institute for Solid State Physics and Optics, Hungarian Academy of Sciences

(**) E-mail: Helmut.Ritsch@uibk.ac.at

spontaneous emission is in the core of the cooling process. This has of course the immediate consequence of heating by momentum diffusion and density limitations due to reabsorption. Moreover, the extra lasers and optics needed for the cooling pose severe restrictions in really microscopic setups.

In this Letter we investigate an efficient method for loading and cooling atoms in a bichromatic evanescent-wave dipole trap. As a main virtue of our scheme, there is no need of the atom to change its internal state or undergo spontaneous emission. The two evanescent field modes, in addition to producing the optical potential trap, simultaneously take over the role of a dissipation channel for the kinetic energy of the atoms. The system relies on a *dynamic* trapping field that imposes a nonconservative motion on an atom. A central requirement to implement this scheme is a significant coupling between the field modes and the atomic dipole. This implies a geometry with the two fields being confined in small mode volumes, which can be achieved with monolithic resonators (microspheres, microdisks, hollow fibers).

In the strong atom-field coupling regime the dynamical behaviour of the system is rather complex. The atom moves guided by the dipole force potential but at the same time acts as a moving refractive index with a non-negligible effect on the field dynamics. As a consequence the field amplitudes depend on the atomic position. A coupled dynamics arises in which the atom can be damped via the cavity field decay [11–13]. The basic mechanism responsible for the kinetic energy loss can be elucidated on the simple example of an atom colliding with a single blue-detuned evanescent field at a given surface. For suitable parameters, the photon numbers in the repulsive field may vary such that the atom approaching the surface climbs a higher wall than the one it is repelled from when moving away. Such a bounce can be viewed as a Sisyphus-type process with photon number states replacing the atomic hyperfine states. The only further necessary ingredient in our system is now a second long-range attractive field which pulls the atoms repeatedly towards the surface. In principle this system can form a 3D trap. For simplicity and in order to work out the basic principles, we will, however, investigate a generic 1D version of such a trap where both the attractive and repulsive fields are dynamic.

The model system under consideration is schematically represented in figure 1. We restrict the atomic motion to one spatial dimension x perpendicular to the surface. The incidence angles of the totally reflected fields are adjusted such that the penetration depth of the blue field (b) is just the half of that of the red one (r), with frequencies properly chosen to match the specific atomic level scheme. The field mode functions above the surface are given simply by $f_r(x) = \exp(-kx)$ and $f_b(x) = \exp(-2kx)$ for the modes r and b , respectively. The two modes are assumed to couple to different dipole transitions in the atom. Their frequencies are sufficiently detuned from the atomic transition to reduce atomic excitation and spontaneous emission. The atom-field detuning is chosen Δ_A for both dipole transitions but with opposite signs for the 'red' and 'blue' fields. The frequencies of the actual red and blue fields are also detuned from the cavity resonances. These pump-mode detunings are set to the same negative value Δ_C many orders of magnitude less than Δ_A (scheme in figure 1 is not to scale). For the sake of simplicity, the mode linewidth κ and the atomic linewidth γ , as well as the dipole coupling constant g , are assumed to be the same for both fields and we consider strong coupling, i.e., g being of the same order of magnitude as κ and γ . This is about an order of magnitude less than it could be in specific microsphere setups [14, 15] but still fairly large. Although a higher g would improve the system performance, we aim to demonstrate that the actual "top" value of g is not absolutely necessary. Indexing the quantities Δ_C , Δ_A , g , κ , γ would unnecessarily complicate the notation without adding new physical effects. As a numerical example we set $\gamma = 2 \times 10^7 \text{ s}^{-1}$, $\kappa = \gamma/2$, $g = 2.5\gamma$, $\Delta_C = -0.8\kappa$, $\Delta_A = 10^3\gamma$ and $k^{-1} = 0.3\mu\text{m}$.

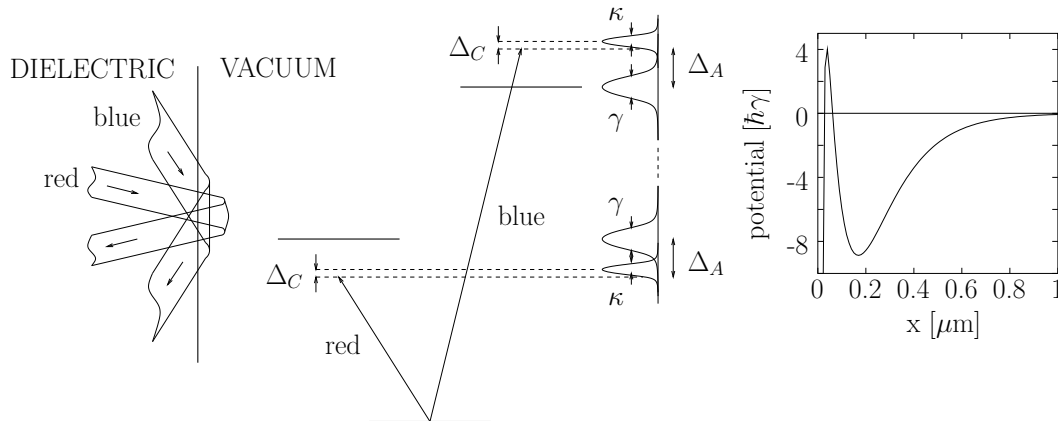


Fig. 1 – Left: The geometrical arrangement of the beams. The penetration depth of the blue is just the half of that of the red field. Center: Excited transitions and detunings, not to scale, involved in the scheme. Right: The adiabatic potential for the atomic motion, including the strong Van der Waals attraction of the surface.

Having fixed the detunings, the only remaining control parameters are the pump strengths η_i ($i = r, b$) of the two modes and normalized such that $|\eta_i|^2/(\Delta_C^2 + \kappa^2)$ gives the stationary photon number in the mode i when no atoms are present. The intensity of pumping is limited by the low saturation assumption for the atomic transition, i.e the photon number in the fields must be well below the saturation photon number of the atomic transitions, $(\Delta_A^2 + \gamma^2)/2g^2$. In this limit we can associate two independent dipoles with the two transitions. These atomic dipoles being analogous to a microscopic dielectric medium shift the resonance frequency of the interacting mode and incoherently scatter photons out of this mode. The spatial dependence of the coupling between atom and fields follows the exponential mode function. Hence the stationary cavity photon number varies with the atomic position. For a sufficiently slow atom the effect exerted by the nonresonant field can be incorporated into an effective “adiabatic” optical potential. This potential resulting from the red and blue fields is plotted in figure 1 for the given parameter settings. The pumping constants have been set to $\eta_r = 1200$ and $\eta_b = 1500$, giving rise to photon numbers 8800 and 13700 for empty modes, respectively, and limiting maximum saturation 10 %. Although with these intensities the atom is kept far enough from the surface (65nm), we take the conservative Van der Waals attraction into account. Numerically we use $U_{\text{vdw}} = 5 \times 10^{-3}/x^3$, characteristic of the ground state of the ^{85}Rb [16] which is a possible candidate for the atomic system with its $^2\text{S}_{1/2} \leftrightarrow 5^2\text{P}_{3/2}, 5^2\text{P}_{1/2}$ transitions at 780 and 795 nm, respectively (the penetration constants k and $2k$ can be then achieved with 48.3° and 63.5° incidence angles in a $n=1.45$ refractive index medium).

Let us now qualitatively discuss the process of capturing and cooling an atom. Far from the surface an atom feels mainly an attractive force due to the long range red detuned field. Approaching the surface, the atom shifts both mode resonances. The blue detuned mode frequency is pushed to higher, the red one to lower values (the atom is in the ground state). Since the detuning Δ_C is negative, the photon number in the blue field decreases while it increases in the red one. As a consequence the effective potential energy decreases. However, the field amplitude variation cannot follow instantaneously the atomic motion. This time

delay due to the finite response time $1/\kappa$ of the modes is the crucial reason for the resulting nonconservative atomic motion. The potential energy decrease comes to effect slightly after the bounce. On its way out, the atom is subject to a weaker blue detuned field and a stronger red detuned field as compared to its way in. Therefore, as outlined in the introduction, in each atom-surface collision the atom loses a small fraction of its kinetic energy. It cannot escape after the first bounce and can finally be held for long periods in the trap. The trapping time is limited only by extra heating processes (background collisions) or spontaneous emission which, owing to the low saturation, is relatively small.

Let us now turn to a more accurate simulation of the system based on a semiclassical model established recently in ref. [17]. A central simplification in treating the interaction of the atomic dipole with the field modes is the adiabatic elimination of the internal atomic dynamics. This can safely be done if we assume large atom-pump detuning, $\Delta_A \gg g, \gamma$. The effect of the atom in this limit can be regarded as a moving linearly polarizable particle (atom or molecule) with dispersive and absorptive properties given by:

$$U_0 = \frac{g^2 \Delta_A}{\Delta_A^2 + \gamma^2}, \quad \Gamma_0 = \frac{g^2 \gamma}{\Delta_A^2 + \gamma^2}. \quad (1)$$

In this simple model the dipole effect is identical for the red r and blue b fields. With the numerical example considered here $U_0 = 0.0125\kappa$, i. e., the atomic perturbation is very small compared to the linewidth; hence the detuning Δ_C needed to adjust the pumping frequency to a steep enough slope of the spectral line of the cavity mode. The spontaneous scattering rate $\Gamma_0 \approx 10^{-4}$ is negligible compared to other frequencies of the system.

In a further approximation we treat the atomic center-of-mass motion semiclassically. This is a good approximation as long as the atom is well localized in both position and momentum space. It can be fulfilled when $\hbar k^2/M\gamma < 1$. Of course the semiclassical treatment gets invalid if the atom is cooled to the lowest few bound quantum states of the trap. In ref. [17] we showed that the consistent treatment of the noise (momentum diffusion) requires additionally an approximate quantum description of the field. In our case, this is very well fulfilled since photon numbers on the order of 10^4 are involved.

A set of coupled, stochastic differential equations can now be established to simulate the dynamics:

$$\begin{aligned} \dot{x} &= \frac{p}{M}, \\ \dot{p} &= -\hbar U_0 \left(|\alpha_r|^2 - \frac{1}{2} \right) \nabla f_r^2(x) - \hbar U_0 \left(|\alpha_b|^2 - \frac{1}{2} \right) \nabla f_b^2(x) + \xi_p, \\ \dot{\alpha}_r &= \eta_r + i \left(\Delta_C - U_0 f_r^2(x) \right) \alpha_r - \left(\kappa + \Gamma_0 f_r^2(x) \right) \alpha_r + \xi_{\alpha_r}, \\ \dot{\alpha}_b &= \eta_b + i \left(\Delta_C - U_0 f_b^2(x) \right) \alpha_b - \left(\kappa + \Gamma_0 f_b^2(x) \right) \alpha_b + \xi_{\alpha_b}, \end{aligned} \quad (2)$$

where the variables x and p represent the position and the momentum of the atomic center-of-mass, α_r and α_b denotes the complex field amplitudes of the red and blue fields, respectively. The terms ξ represent the noise and are defined via the diffusion coefficients:

$$\begin{aligned} \langle \xi_{\alpha_i}^* \xi_{\alpha_i} \rangle &= \frac{1}{2} \left(\kappa + \Gamma_0 f_i^2(x) \right), \\ \langle \xi_p \xi_p \rangle &= \sum_{i=r,b} 2\Gamma_0 \left(|\alpha_i|^2 - \frac{1}{2} \right) \left((\hbar \nabla f_i(x))^2 + \hbar^2 k_i^2 u^2 f_i^2(x) \right), \end{aligned} \quad (3)$$

with $i = r, b$. While the first term of the momentum diffusion coefficient represents dipole heating, the second term accounts for momentum fluctuations due to the random direction

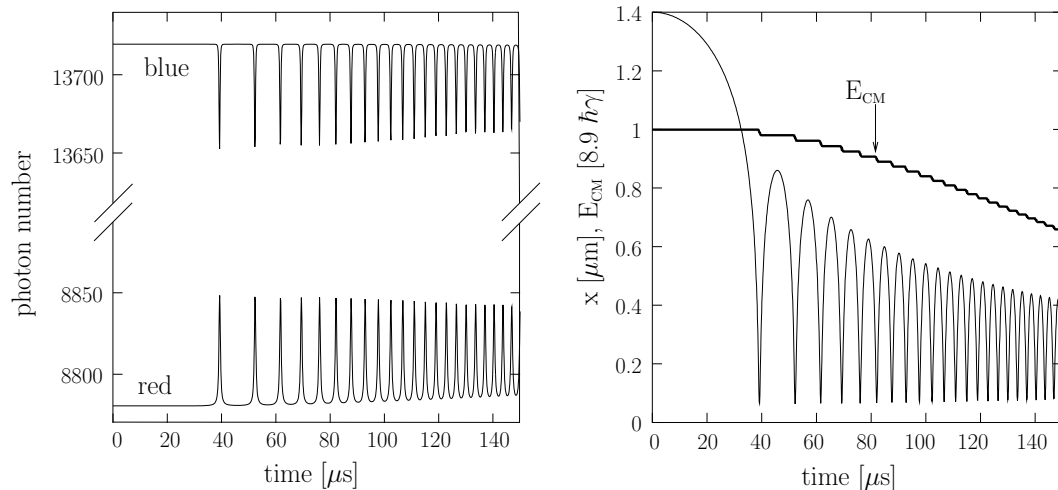


Fig. 2 – Left: Variation of the photon numbers in the blue and red detuned modes. Right: Oscillations in the trap with decreasing amplitude. Bold line represents the mechanical energy of the atom including the kinetic energy and the adiabatic potential energy. The scale for this curve assumes the units of the trap depth that is about $8.9 \hbar\gamma$.

of spontaneously emitted photons. Here k_i corresponds to the wavevector of the transition quiresonant with $i = r$ and $i = b$ fields. The factor u^2 is characteristic of the angular distribution of spontaneous emission. Note that both terms are proportional to Γ_0 and decrease for larger detunings. Surprisingly, the noise terms associated with the momentum and the field amplitudes are correlated:

$$\langle \xi_{\alpha_i} \xi_p \rangle = i\Gamma_0 \alpha_i \hbar f_i(x) \nabla f_i(x), \quad i = r, b. \quad (4)$$

It is instructive to first solve these equations without noise to gain some insight into the cooling mechanism resulting from the coupled atom-field dynamics. In figure 2 we plot the time evolution of important quantities in the dynamics. The photon numbers in the red and blue detuned fields exhibit sharp anticorrelated peaks. The most drastic changes happen at the time duration when the atom is close to the inner turning points and feels the strongest acceleration, while the time evolution is smoother at the outer turning points. After a bounce the photon numbers return relatively fast to the steady-state value. Then the atomic motion becomes approximately conservative in the potential presented in figure 1. The bold line in figure 2 (right side) represents the motional energy associated with the atomic center-of-mass motion (kinetic and potential energy). We clearly see a stepwise decrease of the energy at each inelastic reflection, in agreement with our previous qualitative explanation. For this plot the units are scaled by the depth of the effective potential $8.9 \hbar\gamma$. The energy loss in a single bounce is about $0.17 \hbar\gamma$, which also indicates how large can the initial velocity be (about 7 cm/s) such that the cooling mechanism still leads to trapping after a single bounce.

Figure 3 presents the time evolution including noise sources. In the left graph we selected a trajectory of an atom trapped for a long period. The evolution of the position resembles to the result plotted in figure 2, however, the amplitude of the oscillations takes up some random element. As the oscillations are cooled down, the atom is localized relatively far from the strong field region and the spontaneous photon scattering rate decreases. In some cases the noise causes the atom to leave after the first or eventually after several bounces. Hence a

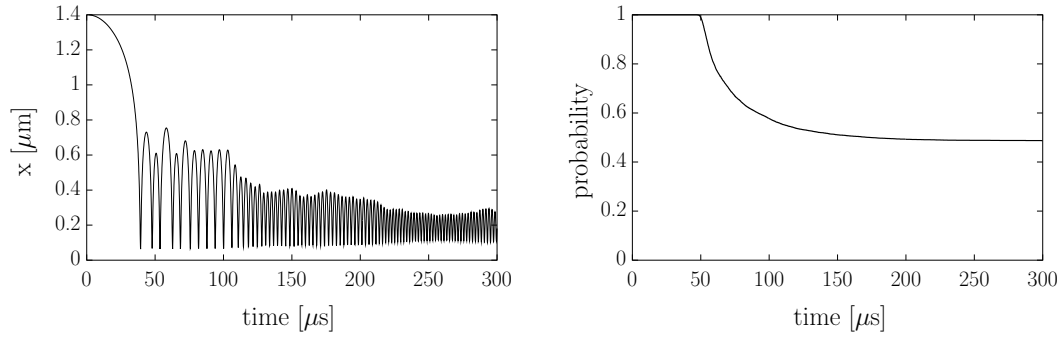


Fig. 3 – Left: Typical trajectory of a trapped atom. Right: The probability of trapping the atom.

very important question is the long-time trapping probability. Figure 3 (right side) shows this trapping probability of an atom as a function of time, averaged over a large number $N=10000$ trajectories. The initial rapid decrease can be attributed to the particles that come too close to the surface in the first bounce or leave the trap due to an incoherent random recoil event during the first cycle. After only very few bouncing times the trapping probability tends to a finite value of 48.5% for the given parameters. Hence an atom which survives the first few bounces will be trapped for a very long time. This provides for a very efficient feeding mechanism of our dynamic evanescent-wave trap. Even on much longer time scales the further decrease of the trapping probability practically vanishes. Figure 4 shows the evolution of the kinetic energy of the atom on a millisecond range. The results from the simulations including and excluding noise have been plotted (this latter stepwise curve is the same as in figure 2). They predict quite similar damping of the atomic kinetic energy. However, in the noiseless case the final state is an atom at rest in the potential minimum, while the noise induces some residual oscillations. In this latter case, the asymptotic kinetic energy corresponds to $\gamma/2.5 \approx \kappa$, which is in good agreement with the results obtained in other cavity configurations [17]. At such a low final temperature, the probability of escaping from the trap is indeed extremely low. In this regime, the actual trapping time might be limited by other mechanisms, such as for example background collisions and technical noise of the apparatus. Also note that,

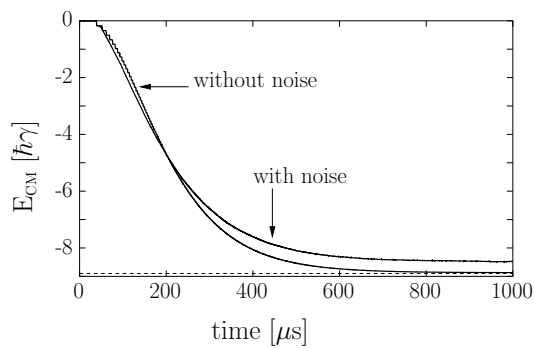


Fig. 4 – The mechanical energy associated with the atomic center-of-mass motion. The result for the noisy dynamics involves an averaging over 10000 trajectories, however, only those are counted that correspond to a trapped atom (48.5 % of the trajectories finally). Dashed line indicates the potential minimum value.

the oscillation frequency in the adiabatic trap being $1.71 \times 10^6 \text{ s}^{-1}$, the final temperature is equivalent to very few (about 4-5) vibrational excitations in the trap. That is, the cooling mechanism is able to drive the atom into the quantized motion regime. Then the semiclassical description is no longer valid and one must resort to a full quantum model involving spatially extended atomic states in the trap.

In conclusion, we calculated the nonconservative motion of an atom in a dynamic optical trap. The probability of capturing an atom from free space has been found to be 48.5 %. The dynamically varying fields can effectively damp the atomic oscillations in the trap, which yields finally very long trapping times limited by technical noise in the setup. A next important step is of course to identify a specific realization of the scheme, and to perform a detailed 3D simulation to calculate the expected performances.

* * *

We thank for the discussions with Peter Horak and Markus Gangl. This work was supported by the Austrian Science Foundation FWF (Project P13435, Z30-TPH Wittgenstein Preis). P. D. acknowledges the financial support by the National Scientific Fund of Hungary under contracts No. T023777 and F032341.

REFERENCES

- [1] BALYKIN V. I., LETOKHOV V. S., OVCHINNIKOV YU. B. and SIDOROV A. I., *Phys. Rev. Lett.*, **60** (1988) 2137
- [2] KASEVICH M. A., WEISS D. S. and CHU S., *Opt. Lett.*, **15** (1990) 607
- [3] AMINOFF C. G., STEANE A. M., BOUYER P., DESBIOLLES P., DALIBARD J. and COHEN-TANNOUJJI C., *Phys. Rev. Lett.*, **71** (1993) 3083
- [4] BARNETT A. H., SMITH S. P., OLSHANI M., JOHNSON K. S., ADAMS A. W. and PRENTISS M., *Phys. Rev. A*, **61** (2000) 023608
- [5] OVCHINNIKOV YU. B., MANEK I. and GRIMM R., *Phys. Rev. Lett.*, **79** (1997) 2225
- [6] GAUCK H., HARTL M., SCHNEBLE D., SCHNITZLER H., PFAU T. and MLYNEK J., *Phys. Rev. Lett.*, **81** (1998) 5298
- [7] OVCHINNIKOV YU. B., SHUL'GA S. V. and BALYKIN V. I., *J. Phys. B: At. Mol. Opt. Phys.*, **24** (1991) 3173
- [8] GORLICKI M., FERON S., LORENT V. and DUCLOY M., *Phys. Rev. A*, **61** (2000) 013603
- [9] OVCHINNIKOV YU. B., LARYUSHIN D. V., BALYKIN V. I. and LETOKHOV V. S., *JETP Lett.*, **62** (1995) 113
- [10] DESBIOLLES P., ARNDT M., SZRIFTGISER P. and DALIBARD J., *Phys. Rev. A*, **54** (1996) 4292
- [11] HORAK P., HECHENBLAIKNER G., GHERI K. M., STECHER H. and RITSCH H., *Phys. Rev. Lett.*, **79** (1997) 4974
- [12] PINKSE P. W. H., FISCHER T., MAUNZ P. and REMPE G., *Nature*, **404** (2000) 365
- [13] HOOD C. J., LYNN T. W., DOHERTY A. C., PARKINS A. S. and KIMBLE H. J., *Science*, **287** (2000) 1447
- [14] TREUSSART F., HARE J., COLLOT L., LEFÈVRE V., WEISS D. S., SANDOGHDAR V., RAIMOND J. M. and HAROCHE S., *Opt. Lett.*, **19** (1994) 1651
- [15] MABUCHI H. and KIMBLE H. J., *Opt. Lett.*, **19** (1994) 749
- [16] LANDRAGIN A., COURTOIS J.-Y., LABEYRIE G., VANSTEENKISTE N., WESTBROOK C. I. and ASPECT A., *Phys. Rev. Lett.*, **77** (1996) 1464
- [17] DOMOKOS P., HORAK P. and RITSCH H., *J. Phys. B: At. Mol. Opt. Phys.*, **34** (2001) 187